

proton transfer with reagents of known proton affinity.

(iv) Adduct formation with ethyl vinyl ether has promise as an analytically useful reaction for screening of epoxide functionalities in small molecules. Further studies on the analytical applications of ion-molecule reactions occurring in the center quadrupole of a triple quadrupole mass spectrometer and a quadrupole ion trap are clearly warranted.

**Acknowledgment.** Dr. M. A. Mabud is thanked for recording the surface-induced dissociation spectra, and Professor R. R. Squires, for the use of his computer program for calculation of experimental collision-activated dissociation threshold energies. Financial support provided by the National Science Foundation (H.I.K.; Grant CHE-8717380) and National Institutes of Health (R.G.C.; Grant CA-33326) is gratefully acknowledged.

## Solid-State Polymerization of Molecular Metal Oxide Clusters: Aluminum 12-Tungstophosphate

A. R. Siedle,<sup>\*,†</sup> Thomas E. Wood,<sup>†</sup> Myles L. Brostrom,<sup>†</sup> David C. Koskenmaki,<sup>§</sup> Bernard Montez,<sup>‡</sup> and Eric Oldfield<sup>‡</sup>

Contribution from 3M Corporate Research Laboratories, 3M Ceramics Technology Center, and 3M Industrial and Electronics Sector Research Laboratory, St. Paul, Minnesota 55144, and School of Chemical Sciences, University of Illinois, Urbana, Illinois 61801.  
Received March 4, 1988

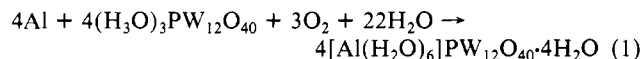
**Abstract:** The molecular metal oxide cluster compound  $[\text{Al}(\text{H}_2\text{O})_6]\text{PW}_{12}\text{O}_{40}\cdot 4\text{H}_2\text{O}$  reversibly dehydrates at 375 °C. Upon heating to  $\geq 550$  °C, irreversible conversion to  $\text{AlPO}_4$  and cubic  $\text{WO}_3$  ( $a = 7.521$  (5) Å) occurs in a solid-state process likened to polymerization. The reaction has been studied by thermogravimetric analysis, differential scanning calorimetry, X-ray and electron diffraction as well as  $^{27}\text{Al}$  and  $^{31}\text{P}$  solid-state NMR. It is proposed as a model for synthesis of ceramics by sol-gel methods.

Chemical ceramics is a generic technology relating to the formation of condensed phase materials, such as metal oxides, from monomeric precursors such as metal alkoxides or aquated metal ions. Embedded in this technology is an underlying chemical question: how can bulk, infinite-lattice materials evolve from molecule-sized species? In one depiction of sol-gel ceramics synthesis, hydrolysis of  $\text{M}(\text{H}_2\text{O})_n^{m+}$  or  $\text{M}(\text{OR})_m$  (M and R are generalized metal and alkyl groups, respectively) yields  $\text{M}-\text{O}-\text{M}$  or  $\text{M}-\text{OH}-\text{M}$  species that, as the hydrolysis proceeds, increase in molecular weight and crosslink density until, ultimately, a recognizable polymer or colloid separates as a new, discrete phase.<sup>1-6</sup> We consider here an alternative scenario, applicable to some metals, in which hydrolysis produces ionic molecular metal oxide clusters that, on heating, condense or polymerize to form bulk oxides.

It has long been known that  $\text{H}_3\text{O}^+$  and group I metal salts of heteropolyanions are thermally unstable and form metal oxides on heating<sup>7-11</sup> by processes that we view not as mere decomposition but as polymerization reactions. Oxide cluster polymerization is taxonomically and logically related to the more familiar polymerization of organic monomers, such as styrene, in the sense that very high molecular weight materials are formed by the combination of a large number of low molecular weight precursors. Polymerization of molecular metal oxide clusters could potentially play an important role in chemical ceramics. In addition, because cluster polymerization occurs at relatively low temperatures (500–600 °C) compared with those usually employed in synthesis of both ceramics and complex oxides, there exists the potential of preparing by this route new, kinetically stable but thermodynamically unstable materials. This paper describes in detail one such exemplary reaction, the solid-state conversion of hydrated aluminum 12-tungstophosphate to  $\text{AlPO}_4$  and the previously unreported cubic form of tungsten trioxide.

### Results and Discussion

Crystalline hydrated aluminum 12-tungstophosphate,  $[\text{Al}(\text{H}_2\text{O})_6]\text{PW}_{12}\text{O}_{40}\cdot 4\text{H}_2\text{O}$ , may be prepared in high purity by reaction of aluminum metal with aqueous  $(\text{H}_3\text{O})_3\text{PW}_{12}\text{O}_{40}$  in air.<sup>12,13</sup> The process differs from many dissolving metal reactions in that hydrogen is not evolved. Instead, aluminum reduces  $\text{PW}_{12}\text{O}_{40}^{3-}$  to a blue heteropolyanion that is subsequently reoxidized by atmospheric oxygen, eq 1. The product separates, after concen-



- (1) Dislich, H. *J. Non-Cryst. Solids* **1983**, *57*, 371.
- (2) *Better Ceramics through Chemistry*; Brinker, C. J., ed. Materials Research Society Symposium Proceedings, Elsevier: New York, NY, 1984; Vol. 32.
- (3) Livage, J.; Lemerle, J. *Ann. Rev. Mater. Sci.* **1982**, *12*, 103.
- (4) Ramsay, J. D. F. *Chem. Soc. Rev.* **1986**, *15*, 335.
- (5) Artaki, I.; Bradley, M.; Zerda, T. W.; Jonas, J. *J. Phys. Chem.* **1985**, *89*, 4299.
- (6) Orgaz, F.; Rawson, H. *J. Non-Cryst. Solids* **1986**, *82*, 57.
- (7) Tsigdinos, G. A. *Ind. Eng. Chem. Prod. Res. Dev.* **1974**, *13*, 267.
- (8) Brown, D. H. *J. Chem. Soc.* **1962**, 3189.
- (9) Rashkin, J. A.; Pierron, E. D.; Parker, D. L. *J. Phys. Chem.* **1967**, *71*, 2165.
- (10) Basu, A. K.; Sale, F. R. *J. Mater. Sci.* **1977**, *12*, 1115.
- (11) West, S. F.; Audreth, L. F. *J. Phys. Chem.* **1955**, *59*, 1069. These workers were among the first to actually examine by X-ray powder diffraction the products of decomposition of  $\text{H}_3\text{O}^+$  Keggin ion salts.
- (12) Preparation of  $\text{AlPW}_{12}\text{O}_{40}$  (degree of hydration not stated) by evaporation "over a water bath" of aqueous  $\text{Al}(\text{NO}_3)_3$  and  $(\text{H}_3\text{O})_3\text{PW}_{12}\text{O}_{40}$  has been reported: Baba, T.; Wanatabe, H.; Ono, Y. *J. Phys. Chem.* **1983**, *87*, 2406. Presumably, a hot water bath was used. No characterization data were given. We find that if the reaction shown in eq 1 is carried out at 50 °C, the product contains impurities demonstrable by additional  $^{31}\text{P}$  NMR peaks.
- (13) A compound described as  $\text{AlPW}_{12}\text{O}_{40}\cdot 13\text{H}_2\text{O}$  has been prepared from  $(\text{H}_3\text{O})_3\text{PW}_{12}\text{O}_{40}$  and  $\text{Al}(i\text{-OC}_3\text{H}_7)_3$ , but no characterization data were given: Hayashi, H.; Moffat, J. B. *J. Catal.* **1983**, *81*, 61. Subsequently, analytical data indicated the composition to be  $\text{Al}_{0.58}\text{H}_{1.26}\text{PW}_{12}\text{O}_{40}$ ; the X-ray powder pattern was analyzed in terms of a cubic unit cell having  $a = 12.135$  Å.<sup>29</sup> On the basis of diffraction data alone, this material differs from the  $[\text{Al}(\text{H}_2\text{O})_6]\text{PW}_{12}\text{O}_{40}\cdot 4\text{H}_2\text{O}$  that we report.

<sup>†</sup> 3M Corporate Research Laboratories.

<sup>‡</sup> 3M Ceramics Technology Center.

<sup>§</sup> 3M Industrial and Electronics Sector Research Laboratory.

<sup>‡</sup> University of Illinois.

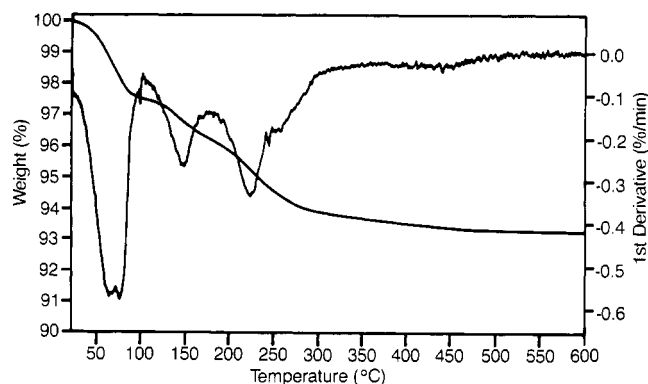


**Figure 1.** Thermogravimetric analysis curve for  $[\text{Al}(\text{H}_2\text{O})_6]\text{PW}_{12}\text{O}_{40} \cdot 4\text{H}_2\text{O}$ .

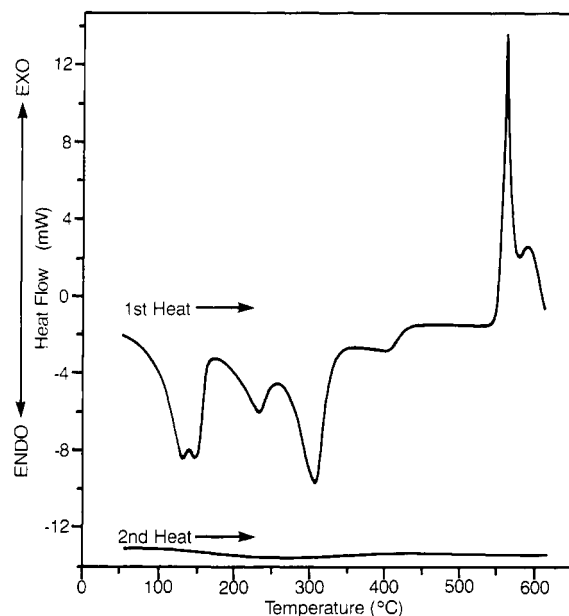


**Figure 2.** Differential thermal analysis data for  $[\text{Al}(\text{H}_2\text{O})_6]\text{PW}_{12}\text{O}_{40} \cdot 4\text{H}_2\text{O}$ . (A). Lower curve (B) was obtained by cooling and then reheating the sample.

tration as colorless crystals. Blue, reduced  $\text{PMo}_{12}\text{O}_{40}^{3-}$  is reoxidized much more slowly by oxygen, and so this approach fails to produce good yields of the molybdenum analogue. Instead,  $[\text{Al}(\text{H}_2\text{O})_6]\text{PMo}_{12}\text{O}_{40} \cdot 7\text{H}_2\text{O}$  was obtained by Dr. Paul Toren of the 3M Corporate Research Laboratories by electrochemical dissolution of an aluminum metal anode in aqueous 12-molybdophosphoric acid. Raman spectra of both compounds are congruent with those of the corresponding  $\text{K}^+$  salts, indicating retention of the Keggin ion structure.<sup>14</sup> The  $^{27}\text{Al}$  magic angle sample spinning (MASS) NMR spectrum of  $[\text{Al}(\text{H}_2\text{O})_6]\text{PW}_{12}\text{O}_{40} \cdot 4\text{H}_2\text{O}$  demonstrates a sharp peak at  $-0.9$  ppm (vide infra). The chemical shift is diagnostic for  $\text{Al}(\text{H}_2\text{O})_6^{3+}$  and justifies the formulation as a hexaaquo aluminum salt.<sup>15</sup> The  $^{31}\text{P}$  and  $^{183}\text{W}$  NMR spectra of a 0.32 M solution in  $\text{D}_2\text{O}$  comprise sharp singlets at  $-17.7$  and  $-96$  ppm, respectively, indicating that no detectable degradation of the  $\text{PW}_{12}\text{O}_{40}^{3-}$  cluster has occurred. The  $^{31}\text{P}$  MASS NMR spectrum displays a sharp resonance at  $-15.9$  ppm.

Thermogravimetric analysis (TGA) of  $[\text{Al}(\text{H}_2\text{O})_6]\text{PW}_{12}\text{O}_{40} \cdot 4\text{H}_2\text{O}$ , Figure 1, shows that loss of water occurs in three stages, i.e., at 70, 150, and 225 °C, and, by 375 °C, the weight loss corresponds to  $10 \pm 0.5$  water molecules per formula weight. The dehydration is reversible for, after the compound had been heated

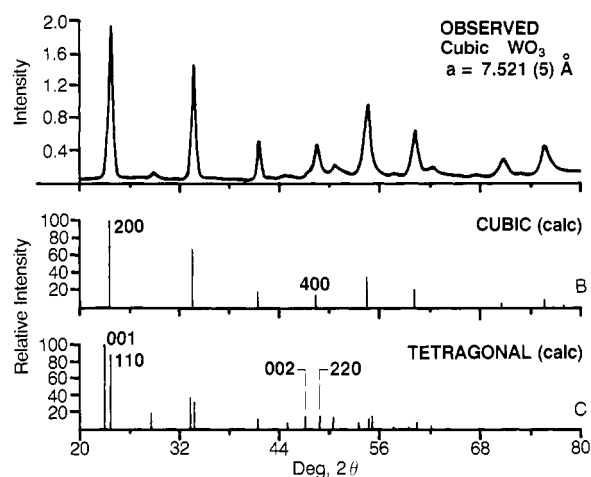


**Figure 3.** (A) X-ray powder diffraction pattern of  $\text{WO}_3$  prepared from  $[\text{Al}(\text{H}_2\text{O})_6]\text{PW}_{12}\text{O}_{40} \cdot 4\text{H}_2\text{O}$ . (B) Pattern of cubic  $\text{WO}_3$  calculated from data in A. (C) Pattern of tetragonal  $\text{WO}_3$  calculated from data in ref 14.

**Table I.** X-ray Powder Diffraction Data for Cubic  $\text{WO}_3$

$d_{hkl}, \text{\AA}$	$I_{\text{rel}}$	$hkl$	$d_{\text{calcd}}, \text{\AA}$
3.761	100	2 0 0	3.7605
2.662	69	2 2 0	2.6591
2.176	20	2 2 2	2.1711
1.878	16	4 0 0	1.8802
1.6803	36	4 2 0	1.6817
1.5348	22	4 2 2	1.5352
1.3305	6	4 4 0	1.3295
1.2538	11	6 0 0	1.2535
		4 4 2	1.2535
1.2232	2	6 1 1	1.2201
		5 3 2	1.2201
1.1876	3	6 2 0	1.1892
1.1299	3	6 2 2	1.1338
1.0880	1	4 4 4	1.0856
1.0420	2	6 4 0	1.0430
1.0049	3	6 4 2	1.0050

to 350 °C and then exposed to air, the Raman spectrum and TGA curve match those of the starting material. Presumably, the aluminum cations in hydrated  $[\text{Al}(\text{H}_2\text{O})_6][\text{PW}_{12}\text{O}_{40}]$  are well separated by the much larger cluster anions; this, and the absence of an efficient proton acceptor would disfavor formation of very stable hydroxy-bridged aluminum species on dehydration. Differential thermal analysis (DTA), cf. Figure 2A, discloses a strong exotherm that is not associated with any weight loss. It represents an irreversible chemical reaction for, after the compound has been heated to 600 °C and cooled, no exotherm appears on reheating, cf. Figure 2B. The free energy of the high temperature process, determined by differential scanning calorimetry (DSC) is large,  $-34 \text{ kcal mol}^{-1}$ , cf. Figure 5A. The DTA and DSC data also reveal that an additional, weakly exothermic reaction occurs at 580 °C. It will be discussed below.

The X-ray powder pattern of  $[\text{Al}(\text{H}_2\text{O})_6]\text{PW}_{12}\text{O}_{40} \cdot 4\text{H}_2\text{O}$  that had been heated at 550 °C for 1 h, Figure 3A, discloses that cubic tungsten trioxide comprises the major crystalline phase. Figure 3B shows the diffraction pattern of cubic  $\text{WO}_3$  calculated from the data in Figure 3A. Figure 3C represents the pattern for  $\text{Nb}_2\text{O}_5$ -stabilized tetragonal  $\text{WO}_3$  calculated by using published lattice constants.<sup>16</sup> It can be seen that distortion from cubic to tetragonal symmetry leads to a doubling of the 200 and 400 reflections which become 001, 110 and 002, 220, respectively, in this lower symmetry. Components of these doubled peaks can be recognized as shoulders in Figure 3A, and their presence indicates that tetragonal  $\text{WO}_3$  is present as a minor phase. Least-squares refinement of 14 observed reflections, Table I, yields the lattice parameter  $a$ ,  $7.521 (5) \text{\AA}$  (cf.  $3.748 \text{\AA}$  for  $\text{ReO}_3$ ).

(14) Pope, M. T. *Heteropoly and Isopoly Oxometallates*; Springer-Verlag: New York, NY, 1983.

(15) Karlik, S.; Tarien, E.; Elgavish, G. A.; Eichorn, G. L. *Inorg. Chem.* **1983**, *22*, 525.

(16) Roth, R. S.; Waring, J. J. *Res. Natl. Bur. Stds.* **1966**, *70A*, 281.

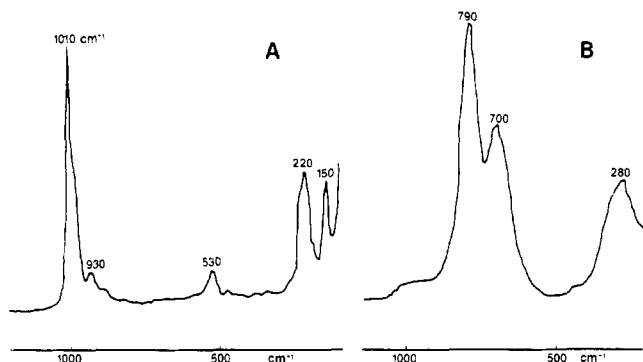


Figure 4. Raman spectra of  $[\text{Al}(\text{H}_2\text{O})_6]\text{PW}_{12}\text{O}_{40} \cdot 4\text{H}_2\text{O}$  before (A) and after (B) heating.

Diffraction lines at 1.0049 and 1.2232 Å are incompatible with the respective alternative unit cell lengths of 5.318 and 3.761 Å (i.e.,  $a\sqrt{2}/2$  and  $a/2$ ), which give rise to calculated diffraction patterns in which lines having these d spacings are absent. Prolonged grinding of the product produced no measurable change in the diffraction pattern, and so the X-ray analysis is not affected by sample preparation. Electron diffraction patterns of thin specimens of the product reveal spot patterns having 6-fold symmetry about the  $\langle 111 \rangle$  zone axis that are characteristic of a cubic lattice; larger aggregates yield ring patterns that are congruent with the spot patterns. Tilting for  $\langle 001 \rangle$  to  $\langle 110 \rangle$  to  $\langle 111 \rangle$  zone axes confirmed the cubic symmetry of the lattice, and analysis of the diffraction spots yielded a lattice parameter of 7.56 (3) Å, in agreement with the X-ray result. In one case, transformation, under the influence of the electron beam, of a very small crystal, having an apparently twinned microstructure, to cubic  $\text{WO}_3$  was observed.<sup>17</sup>

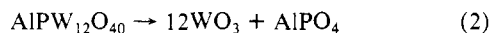
The light yellow, diamagnetic (no EPR spectrum) tungsten oxide produced in this reaction has a surface area of  $16 \text{ M}^2 \text{ g}^{-1}$ . Scanning electron microscopic analysis demonstrates that it consists of a mixture of numerous small (0.08–0.15  $\mu\text{m}$ ) ramified, spheroidal nodules and larger (0.1–0.25  $\mu\text{m}$ ) weakly faceted aggregates that exhibit extensive microcracking. Many fewer nodules are seen littering the surfaces of the  $\geq 30 \mu\text{m}$  crystals of  $[\text{Al}(\text{H}_2\text{O})_6]\text{PW}_{12}\text{O}_{40} \cdot 4\text{H}_2\text{O}$ . This precursor has a surface area of only  $1.1 \text{ M}^2 \text{ g}^{-1}$ . Loss of water on heating and conversion to  $\text{WO}_3$  thus leads to a large increase in surface area by production of many smaller aggregates and of microcracks.

Raman spectroscopy provides further evidence that the Keggin ion structure of the  $\text{PW}_{12}\text{O}_{40}^{3-}$  cluster is lost upon heating. In particular, the characteristic  $\text{W}=\text{O}$  stretching band<sup>18</sup> at  $1010 \text{ cm}^{-1}$  disappears, and the spectrum of the pyrolyzed material matches that of authentic  $\text{WO}_3$ , Figure 4. The sampling scale of vibrational spectroscopy is ca.  $10^{-9} \text{ M}$ , and, thus, the spectra show that conversion is complete and that, within limits of detectability (estimated at  $<3 \text{ wt } \%$ ), regions of unreacted  $\text{AlPW}_{12}\text{O}_{40}$  are not present.

Aluminum phosphate is formed as a coproduct in this reaction. It is, as noted above, not detected by X-ray diffraction because it represents a dilute phase in the midst of a strongly diffracting phase and probably forms as a glassy or poorly crystalline phase. Examination of pyrolyzed  $\text{AlPW}_{12}\text{O}_{40}$  by energy dispersive X-ray analysis provides no evidence for the presence of discrete volumes containing, predominantly,  $\text{AlPO}_4$ . However, it is readily discerned by  $^{27}\text{Al}$  MASS NMR spectroscopy (vide infra). Crystallization of  $\text{AlPO}_4$  does, however, occur on prolonged annealing. For example, in samples heated at  $600^\circ\text{C}$  for 187 h, the characteristic (100) and (102) reflections of the quartz form of  $\text{AlPO}_4$  can be recognized. The "extra" feature at  $580^\circ\text{C}$  in the DSC curve is thus likely associated with this phase, for it is at this temperature that the low quartz to high quartz transition in  $\text{AlPO}_4$  occurs.<sup>19,20</sup>

Conversion of  $\text{AlPW}_{12}\text{O}_{40}$  to  $\text{WO}_3$  and  $\text{AlPO}_4$  has been followed by a combination of differential scanning calorimetry and  $^{27}\text{Al}$  and  $^{31}\text{P}$  solid-state NMR spectroscopy. Bulk samples were heated at  $500^\circ\text{C}$  for 1 and 3 h and at  $600^\circ\text{C}$  for 1 h and then quenched by cooling to room temperature. The DSC for the original material, Figure 5A, and following these heat treatments, Figure 5 (parts C and D), indicate that the reaction is 7, 77, and 100% complete, respectively. The  $^{31}\text{P}$  and  $^{27}\text{Al}$  MASS NMR spectra of heat-treated samples are shown in Figures 6A–D and 7A–D, respectively. As expected from the DSC results, no further changes occur after heating for 1 h at  $600^\circ\text{C}$ . As  $\text{AlPO}_4$  formation proceeds, the sharp  $\text{PW}_{12}\text{O}_{40}^{3-}$  phosphate resonance diminishes in intensity and is replaced by a broad (ca. 20 ppm) signal at  $-14.0 \text{ ppm}$ . The  $^{31}\text{P}$  chemical shift and line width are consistent with the presence of  $\text{AlPO}_4$  in a glassy or poorly ordered phase. The  $^{27}\text{Al}$  spectra are surprising. The initial, relatively sharp peak at  $-0.9 \text{ ppm}$  is replaced by a much broader peak at 40 ppm. The chemical shift of the latter is characteristic of tetrahedral aluminum, as occurs in  $\text{AlPO}_4$ , and is in agreement with other  $^{27}\text{Al}$  NMR data for  $\text{AlPO}_4$ -based molecular sieves.<sup>21</sup> However, regardless of the heat treatment employed, there remains a sharper resonance at 4.3 ppm, in a shift region characteristic of octahedrally coordinated aluminum. Figure 8A reproduces the  $^{27}\text{Al}$  MASS NMR spectrum of  $\text{AlPW}_{12}\text{O}_{40}$  that had been heated for 1 h at  $600^\circ\text{C}$ . The spectrum of the same material, obtained with  $^1\text{H}$  cross polarization, is shown in Figure 8B. Only the 4.3-ppm peak is visible, presumably because it arises from a species having nearby protons. This experiment, together with the chemical shift information, indicates that the higher field  $^{27}\text{Al}$  resonance is due to  $\text{Al}(\text{H}_2\text{O})_6^{3+}$  or, more probably, surface  $\text{Al}-\text{OH}$  groups. We surmise that the latter arise from reaction of poorly crystalline  $\text{AlPO}_4$  with atmospheric moisture. Because the product contains only 2%  $\text{AlPO}_4$ , the amount of water required to hydrate the  $\text{AlPO}_4$  is expected to be small and very difficult to detect by conventional infrared analysis. Our results are consistent with the recent observation by solid-state  $^1\text{H}$  MASS NMR studies of surface  $\text{Al}-\text{OH}$  groups on amorphous aluminum phosphate catalysts.<sup>22,23</sup>

Pyrolysis of  $[\text{Al}(\text{H}_2\text{O})_6]\text{PW}_{12}\text{O}_{40} \cdot 4\text{H}_2\text{O}$  involves initial, reversible dehydration that is complete by  $400^\circ\text{C}$ . At  $>500^\circ\text{C}$ , gross rearrangement of the Keggin ion structure occurs. Conceptually, the globular  $\text{PW}_{12}\text{O}_{40}$  molecular metal oxide cluster can be viewed as unfolding, with ejection of the central  $\text{PO}_4^{3-}$  ion, to give a nearly planar species which undergoes strongly exothermic polymerization to form tungsten oxide. The stoichiometry is given, simplistically, by



and a three-dimensional representation, which has no particular mechanistic implications, is shown in Figure 9. We consider that the polymerization reaction, after thermal initiation at a random site, propagates through the particles of  $\text{AlPW}_{12}\text{O}_{40}$  until halted by a defect or at the edge of the particle (vide infra).

Formation of cubic  $\text{WO}_3$  was followed by monitoring its 200 and 220 reflections as a function of time and temperature, between 500 and  $600^\circ\text{C}$ , by use of an automatic diffractometer equipped with a heating stage. The polymerization reaction is presumably kinetically limited for small amounts of  $\text{WO}_3$  are detectable at as low as  $500^\circ\text{C}$  even though this temperature is well below that of the large exotherm at  $550^\circ\text{C}$ . The two  $\text{WO}_3$  reflections were narrow, having peak widths of  $0.43 (1)^\circ$  in  $2\theta$ , and remained so during the course of the reaction. Therefore, the  $\text{WO}_3$  that forms even in the initial stages of the reaction is crystalline, a situation

(19) Muller, O.; Roy, R. *The Major Ternary Structural Families*; Springer-Verlag: New York, NY, 1974; p 121.

(20) Ng, H. N.; Calvo, C. *Can. J. Phys.* **1976**, *54*, 638.

(21) Blackwell, C. S.; Patton, R. L. *J. Phys. Chem.* **1984**, *88*, 6135.

(22) Mastikhin, V. M.; Mudrakovsky, I. L.; Shmachkova, V. P.; Kotsarenko, N. S. *Chem. Phys. Lett.* **1987**, *139*, 93.

(23) (a) Volpe, L.; Boudart, M. *Catal. Rev.-Sci. Eng.* **1985**, *27*, 515. (b) Thomas, J. M.; Morsi, S. E.; Desvergne, J. P. *Adv. Phys. Org. Chem.* **1977**, *15*, 63. (c) Gazevotti, A.; Simonetta, M. *Chem. Rev.* **1982**, *82*, 1.

(17) Sahle, W. *J. Solid State Chem.* **1982**, *45*, 324.

(18) Rocchiccioli-Deltchev, C.; Thouvenot, R.; Dababbi, M. *Spectrochim. Acta* **1977**, *33A*, 143.

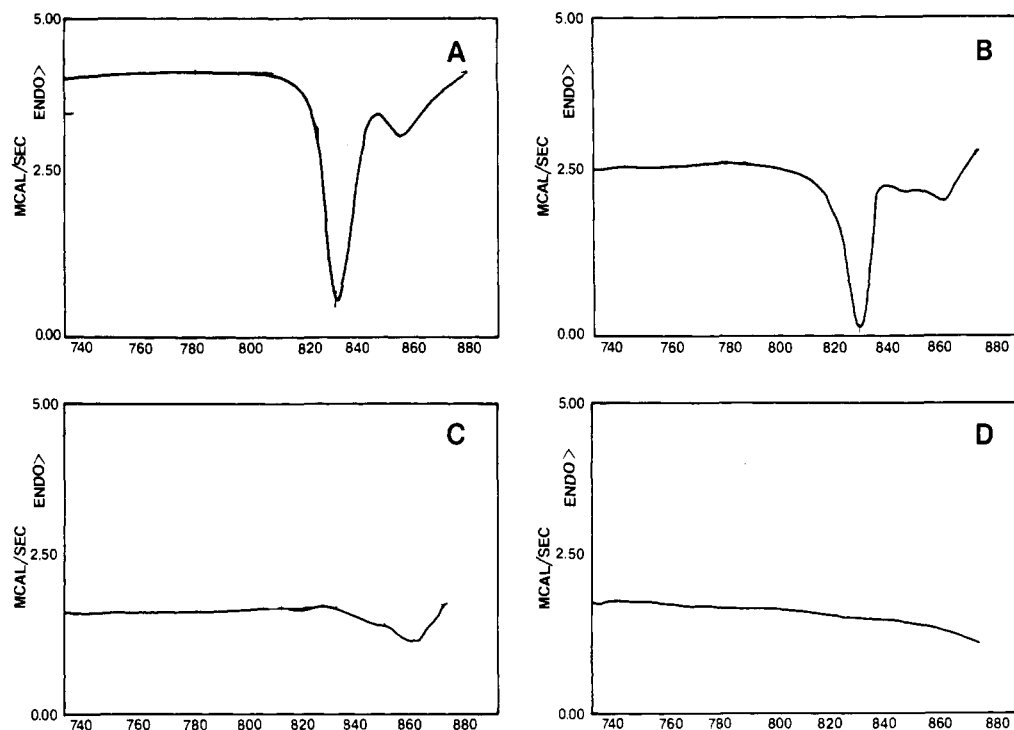


**Figure 5.** Differential scanning calorimetry curves for  $[\text{Al}(\text{H}_2\text{O})_6]\text{PW}_{12}\text{O}_{40}\cdot 4\text{H}_2\text{O}$ : (A) as synthesized; and after heating to 500 °C for 1 h (B), 500 °C for 3 h (C), and 600 °C for 1 h (D).

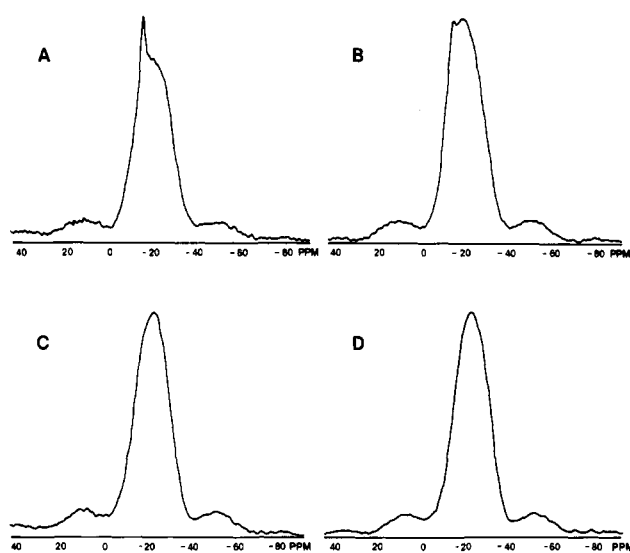


**Figure 6.** 201 MHz  $^{31}\text{P}$  MASS NMR spectra of  $[\text{Al}(\text{H}_2\text{O})_6]\text{PW}_{12}\text{O}_{40}\cdot 4\text{H}_2\text{O}$  after heating at 500 °C for 1 h (A), 500 °C for 3 h (B), 600 °C for 1 h (C), and 600 °C for 3 h (D).

that would likely not obtain if this oxide were formed at multiple nucleation sites, followed by recrystallization and grain growth.<sup>24</sup>

Tungsten oxide has a quite complex crystal chemistry, the monoclinic(I), triclinic, monoclinic(II), orthorhombic, and tetragonal forms being related via a series of phase transitions. All polymorphs apparently represent subtle distortions from the cubic  $\text{ReO}_3$  structure that are associated with small cation displacements.<sup>16,25-27</sup> Formation of cubic  $\text{WO}_3$  from  $\text{AlPW}_{12}\text{O}_{40}$  is

(24) A reviewer has suggested that formation of  $\text{Al}_2(\text{WO}_4)_3$  might occur. This is certainly possible [cf. Levin, E. M.; Robbins, C. R.; McMurdie, H. F. *Phase Diagrams for Ceramicists 1919 Supplement*; American Ceramic Society: Columbus, OH, 1969; p 97, Figure 2350] if the system were at thermodynamic equilibrium, which it is not. We observe no characteristic X-ray powder diffraction lines for  $\text{Al}_2(\text{WO}_4)_3$ . In this compound, aluminum has an octahedral coordination geometry, and no  $^{27}\text{Al}$  resonances for it are observed, cf. -11.8 and -14.9 ppm for  $\text{Al}_2(\text{MoO}_4)_3$ .

(25) McCarron III, E. M. *J. Chem. Soc., Chem. Commun.* **1986**, 336.

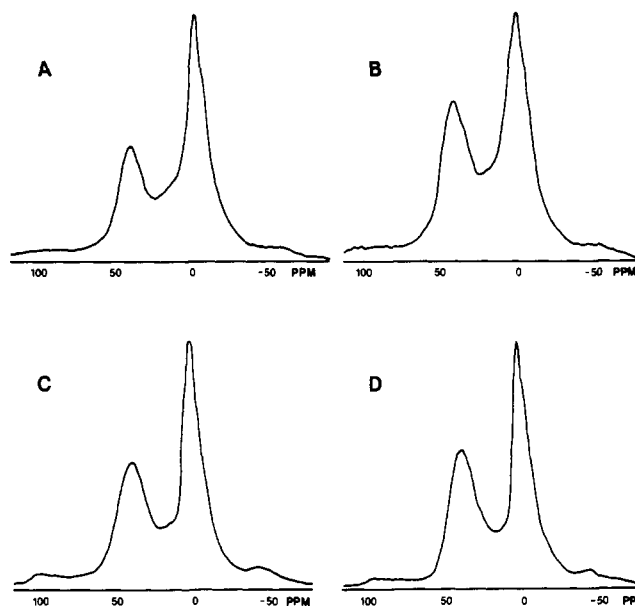


**Figure 7.** 131 MHz  $^{27}\text{Al}$  MASS NMR spectra of  $[\text{Al}(\text{H}_2\text{O})_6]\text{PW}_{12}\text{O}_{40}\cdot 4\text{H}_2\text{O}$  after heating at 500 °C for 1 h (A), 500 °C for 3 h (B), 600 °C for 1 h (C), and 600 °C for 3 h (D).

surprising, and we are unaware of any previous characterization of this high-symmetry polymorph. Stabilization of the cubic form is not associated with the mere presence of phosphorus in the heteropolyanion. Pyrolysis of  $(\text{NH}_4)_3\text{PW}_{12}\text{O}_{40}\cdot 13\text{H}_2\text{O}$  at 600 °C yields orthorhombic  $\text{WO}_3$ ,<sup>28,29</sup> the unit cell parameters derived

(26) (a) Wells, A. F. *Structural Inorganic Chemistry*, 5th ed.; Oxford University Press: New York, NY, 1984; p 572. (b) Rao, C. N. R. *Solid State Chemistry*; Dekker: New York, NY, 1974; p 528.

(27) Salje, E. *Acta Crystallogr.* **1977**, B33, 574.

(28) Decomposition of  $(\text{H}_3\text{O})_3\text{PW}_{12}\text{O}_{40}$  is reported to yield a tetragonal phosphate-stabilized  $\text{WO}_3$  phase, cf.: Varfolomeev, M. B.; Burljaev, V. V.; Toporenskaja, T. A.; Lunk, H.-J.; Wilde, W.; Hilmer, W. *Z. Anorg. Allg. Chem.* **1981**, 472, 185. We have repeated this work and confirm that the product produced by heating to 650 °C for 2 h is tetragonal, having  $a = 5.30$  and  $c = 3.83$  Å. The product, after heating at 550 °C for 2 h, gives rise to a cubic-type X-ray diffraction pattern like that in ref 9.

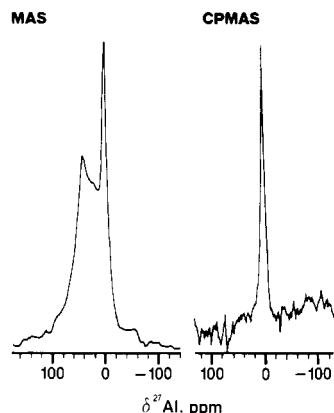


Figure 8. 131 MHz  $^{27}\text{Al}$  MASS NMR spectra of  $[\text{Al}(\text{H}_2\text{O})_6]\text{PW}_{12}\text{O}_{40}\cdot 4\text{H}_2\text{O}$  after heating at 600 °C for 1 h obtained without (left) and with (right)  $^1\text{H}$  cross polarization.

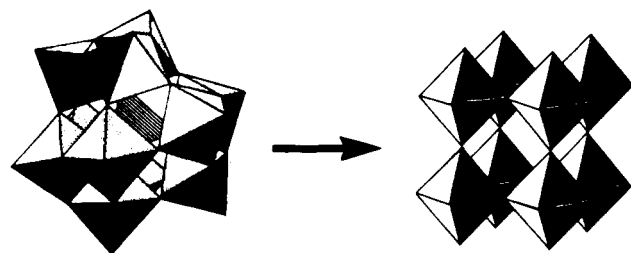


Figure 9. Conceptual view of  $\text{PW}_{12}\text{O}_{40}^{3-}$  cluster polymerization to form a fragment of the bulk  $\text{WO}_3$  lattice.  $\text{Al}^{3+}$  and the central  $\text{PO}_4^{3-}$  ion combine to form  $\text{AlPO}_4$  (not shown).

from refinement of X-ray powder data,  $a = 7.477$  (2),  $b = 7.502$  (3) and  $c = 7.720$  (2) Å, are in good agreement with literature values.<sup>16,25-27</sup> It is not well understood why distortions of the cubic  $\text{WO}_3$  occur so easily, and our results do not establish why the cubic form is produced and stabilized here; it is possible that it is associated with the presence of aluminum although attempts to prepare the cubic phase by doping are reported to have been unsuccessful.<sup>26b</sup> We note, however, that even if aluminum were present in the  $\text{WO}_3$  lattice, it cannot be argued that its presence causes stability. This cubic polymorph is thermodynamically unstable and rearranges upon heating at 1000 °C to form monoclinic  $\text{WO}_3$ . Obtention of this metastable form of  $\text{WO}_3$  is due, in part, to the mild, low-temperature conditions under which  $\text{AlPW}_{12}\text{O}_{40}$  polymerization occurs. The chemistry of  $\text{AlPW}_{12}\text{O}_{40}$  differs markedly from that of  $\text{AlH}[\text{SiW}_{12}\text{O}_{40}]\cdot 29\text{H}_2\text{O}$  which is reported to yield  $(\text{Al}_2\text{O}_3)_{0.5}\text{SiO}_2\cdot (\text{WO}_3)_{12}$  when heated at 500 °C.<sup>30</sup>

Thermal polymerization of  $[\text{Al}(\text{H}_2\text{O})_6]\text{PMo}_{12}\text{O}_{40}\cdot 7\text{H}_2\text{O}$  has been studied in less detail, but its chemistry parallels that of the tungsten analogue. Thermogravimetric analysis shows that water loss occurs in stages, i.e., at 80, 107, and 250 °C. DSC analysis discloses that conversion to orthorhombic  $\text{MoO}_3$  is associated with a strong exotherm at 397 °C, corresponding to a free energy change of  $-27.2$  kcal mol $^{-1}$ .

From the results presented above, we conclude that, on heating, the aluminum salts of  $\text{PW}_{12}\text{O}_{40}^{3-}$  and  $\text{PMo}_{12}\text{O}_{40}^{3-}$  are converted to  $\text{AlPO}_4$  and  $\text{WO}_3$  or  $\text{MoO}_3$ . The formation of these bulk, condensed phase oxides from molecular metal oxide precursors exhibits some of the characteristics, taxonomic at least, of polymerization of purely organic monomers. Viewed in this way,

the structures of the clusters and of the product oxides are seen to be related. Further, because molecular metal oxide polymerization proceeds at relatively low temperatures, synthesis of kinetically stable but thermodynamically unstable oxides, here exemplified by cubic  $\text{WO}_3$ , can be effected.

Other elements besides Mo and W, such as Al, Fe, V, Nb, Ta, and Zr, are known to form polyoxoanions. These clusters contain the metals in high or maximal valence states and are readily produced in water under conditions of temperature and pH appropriate to synthesis of ceramics by sol-gel methods. Oxide cluster polymerization chemistry may, in favorable cases, provide useful routes to, and experimentally tractable models for, more complex, technologically important systems as well as to new materials.

## Experimental Section

Thermogravimetric analyses and differential scanning calorimetry experiments were performed on Perkin Elmer TGS-7 and DSC-2C instruments. The heating rates, in air, were 10 and 20 °C min $^{-1}$ , respectively. Differential thermal analyses were carried out with a du Pont 1200 instrument. Raman spectra were obtained on powdered samples in glass capillaries with 5145 Å excitation.

$^{31}\text{P}$  and  $^{183}\text{W}$  NMR solution phase spectra were recorded on a Varian XL-400 spectrometer. Chemical shifts are expressed relative to external 85%  $\text{H}_3\text{PO}_4$  or 2 M  $\text{NaWO}_4$  in  $\text{D}_2\text{O}$ , respectively.  $^{27}\text{Al}$  and  $^{31}\text{P}$  MASS NMR spectra were obtained on a FTNMR spectrometer operating at 131 and 201 MHz, respectively, with an Oxford Instruments 11.7 Tesla, 52 mm bore superconducting solenoid magnet. A Nicolet Instrument Corp. Model 1280 computer system was used for data acquisition and Amplifier Research Model 200L and 150LA amplifiers for RF pulse generation. Spectra were obtained with a 5 mm Doty probe or a home-built "windmill" design probe.  $^{27}\text{Al}$  chemical shifts refer to the position of the peak maxima in the spectra. Positive chemical shifts are to low field of the external references, 1 M  $\text{AlCl}_3$  or 85%  $\text{H}_3\text{PO}_4$ .

X-ray powder diffraction data were collected to  $\geq 60^\circ$  in  $2\theta$  on a Philips APD3600 automatic diffractometer equipped with a temperature controller, a platinum heating stage, and a copper target. Silicon was used as an internal standard to establish line positions. Electron diffraction data were obtained with a JEOL 200CX transmission electron microscope operated at 200 kV.

**$[\text{Al}(\text{H}_2\text{O})_6]\text{PW}_{12}\text{O}_{40}\cdot 4\text{H}_2\text{O}$ .** Hydrated 12-tungstophosphoric acid (Alfa Products), 16 g, 0.16 g of aluminum foil, several glass chips, and 30 mL of distilled water were stirred at room temperature for 3 days. Most of the aluminum had dissolved by then, and a small amount of amorphous white solid separated. The reaction mixture was filtered through a fine porosity glass frit and then concentrated to ca. 5 mL on a rotary vacuum evaporator. After cooling in an ice bath, the colorless crystalline product was isolated by filtration. The yield, after drying in air at 30 °C, was 8.5 g. Anal. Calcd (found) Al, 0.9 (0.7); P, 1.0 (1.1); W, 71.5 (71.9);  $\text{H}_2\text{O}$ , 5.8 (6.0, by TGA). The X-ray powder pattern was indexed in terms of an orthorhombic unit cell having  $a = 30.22$  (1),  $b = 23.77$  (1), and  $c = 22.84$  (1) Å.

Preparation of the aluminum salt of 12-molybdophosphoric acid without addition of extraneous ions was accomplished by electrochemical dissolution of an aluminum anode in aqueous  $(\text{H}_3\text{O})_3\text{PMo}_{12}\text{O}_{40}$ . The electrolysis was carried out in a divided cell at constant current and was terminated after the passage of current coulometrically equivalent to the amount of aluminum required. Contaminant-free  $[\text{Al}(\text{H}_2\text{O})_6]\text{PMo}_{12}\text{O}_{40}\cdot 7\text{H}_2\text{O}$  was isolated by rotary evaporation of the solvent until crystals appeared, chilling in an ice bath, and filtration. The product was then air dried at room temperature. The yield from 2.1 g hydrated  $(\text{H}_3\text{O})_3\text{PMo}_{12}\text{O}_{40}$  was 0.56 g. Anal. Calcd (found): Al, 1.3 (1.1); P, 1.5 (1.5); Mo, 55.2 (54.7);  $\text{H}_2\text{O}$ , 11.2 (11.2, by TGA).

**Acknowledgment.** We are grateful to members of the 3M Analytical and Properties Research Laboratory for spectroscopic and analytical data and particularly to W. T. Conway and David Markoe for the thermal analysis results. NMR experiments performed at the University of Illinois were supported by the Solid State Chemistry Program of the National Science Foundation (Grant DMR 86-15206).

(29) Highfield, J. G.; Moffat, J. B. *J. Catal.* **1984**, *88*, 1984.

(30) Lunk, H.-J.; Varfolomeev, M. B.; Samraj, N. B.; Muller, D.; Hilmer, W. Z. *Anorg. Allg. Chem.* **1986**, *537*, 207.